ISSN 0030-400X, Optics and Spectroscopy, 2013, Vol. 115, No. 6, pp. 858–862. © Pleiades Publishing, Ltd., 2013.
Original Russian Text © I.S. Rodina, A.N. Kravtsova, A.V. Soldatov, G.E. Yalovega, Yu.V. Popov, N.I. Boyko, 2013, published in Optika i Spektroskopiya, 2013, Vol. 115, No. 6, pp. 962–966.

CONDENSED-MATTER SPECTROSCOPY

X-Ray Spectroscopic Identification of Garnet from the Placer Deposits of the Taman Peninsula

I. S. Rodina[a], A. N. Kravtsova[a, b, *], A. V. Soldatov[a, b], G. E. Yalovega[b], Yu. V. Popov[c, d], and N. I. Boyko[c]

[a] *Research Center for Nanoscale Structure of Matter, Southern Federal University, Rostov-on-Don, 344090 Russia*

[b] *Faculty of Physics, Southern Federal University, Rostov-on-Don, 344090 Russia*

**e-mail: akravtsova@sfedu.ru*

[c] *Faculty of Geology and Geography, Southern Federal University, Rostov-on-Don, 344090 Russia*

[d] *Mineral Raw Materials and Environment Status Research Mixed-Use Center, Southern Federal University, Rostov-on-Don, 344090 Russia*

Received March 18, 2013

Abstract—Garnet from recent placer deposits of the Taman peninsula has been investigated by energy-dispersive X-ray fluorescence microanalysis and X-ray absorption near-edge structure (XANES) spectroscopy. Energy-dispersive X-ray fluorescence microanalysis showed that the chemical composition of the garnet under study corresponds to pyrope–almandine–spessartine series. The Fe *K*-edge X-ray absorption spectra of garnet have been recorded using a Rigaku R-XAS laboratory spectrometer. Iron *K*-edge XANES spectra for two iron-containing garnet minals (components), almandine and andradite, have been calculated using the full multiple-scattering and finite-difference methods. Based on a comparison of the experimental and theoretical Fe K-XANES spectra, it is concluded that recent magnetite–garnet placer deposits of the Taman peninsula contain garnet in the form of almandine.

DOI: 10.1134/S0030400X13120163

INTRODUCTION

Minerals the composition and structure of which play the role of indicators of thermodynamic parameters of a mineral-formation medium have been actively investigated to reconstruct the geological processes in the Earth's crust and upper mantle [1–4]. These minerals include garnets, which form a group interrelated by isomorphous substitutions, with the general formula $A_3B_2(SiO_4)_3$, where A = Mg^{2+}, Fe^{2+}, Ca^{2+}, Mn^{2+}, or Y^{2+} and B = Al^{3+}, Fe^{3+}, Cr^{3+}, V^{3+}, Mn^{3+}, Ti^{4+}, or Zr^{4+}. In this paper, we report the results of studying the garnet from recent placer deposits of the Taman peninsula by X-ray-fluorescence (XRF) spectroscopy and X-ray-absorption fine-structure (XAFS) spectroscopy.

X-ray absorption spectroscopy [5, 6] is an efficient method for studying the local atomic structure and electronic subsystem of materials, including those characterized by the absence of long-range order in the atomic arrangement. It is generally accepted to separate the X-ray absorption fine structure into two regions: X-ray absorption near-edge structure (XANES) and extended X-ray absorption fine structure (EXAFS) [7]. EXAFS spectroscopy makes it possible to determine the atomic radial distribution function around an absorbing atom with a fairly high accuracy. XANES spectroscopy has a number of advantages over EXAFS spectroscopy, because it allows one to find not only bond lengths, but also bond angles, i.e., to obtain complete (three-dimensional) information about the local structure of the environment of atoms under study in a specific material.

Obtaining structural data from XANES spectra is a rather difficult problem, which often calls for complicated calculations. Since the formation of fine structure in XANES spectra is affected by many factors, they were previously difficult to interpret. Recently, some progress has been made in the development of theoretical approximations for interpreting XANES data [8, 9]. For example, the number of calculated X-ray absorption spectra can be reduced in some cases using the technique of theoretical analysis of XANES spectra for obtaining a three-dimensional local atomic structure based on multidimensional interpolation [10]. Recently, XANES spectroscopy has been successfully applied to analyze the atomic and electronic structures of different classes of materials in a condensed state [11–13], including ones of geological origin [14–16].

XANES spectroscopy can be applied to identify materials using the "fingerprint" method [8], in which the spectrum of a material under study is compared with the spectra of model compounds with a known local atomic structure (or an experimental

spectrum is compared with theoretical spectra calculated for several structural models). Recently, identification of materials based on XANES spectra recorded using high-intensity synchrotron-radiation sources has been widely used. In this study, for the first time we identified garnet from the deposit of the Taman peninsula using a laboratory X-ray absorption spectrometer.

EXPERIMENTAL

The objects of study were garnet samples from recent magnetite–garnet placer deposits of the Taman peninsula.

The qualitative chemical composition of garnet grains was determined on an analytical SPARK-1-2M short-wavelength X-ray spectrometer. X-ray fluorescence full-range spectra of garnet were recorded in the first reflection order with an exposure time of 3 s at an accelerating voltage of 25 kV. Measurements were performed in a wavelength range of 0.9–2.7 Å with a step of 0.001 Å. The sample was rotated during measurement.

The quantitative chemical composition of garnet grains (i.e., the percentage of the main components with trace impurities having concentrations less than 0.1 wt % neglected) and their phase and chemical homogeneity were studied on a VEGA II LMU scanning electron microscope integrated with the INCA Energy 450/XT system of energy-dispersive X-ray fluorescence microanalysis with an X-Act ADD detector. Microanalysis was carried out at an accelerating voltage of 20 kV with a measurement time per point of 120 s; a thin carbon film was deposited on the polished surface of the grains analyzed. Taking into account zonality of the chemical element distribution (which is often noted for natural garnets), the composition homogeneity was estimated based on the spectra accumulated along the profiles intersecting each grain and by elemental mapping of the grain area (using the OXFORD INCA Energy 450 software package).

XANES spectra were recorded on a laboratory Rigaku R-XAS X-ray absorption spectrometer [17]. Previously, a Rigaku R-XAS spectrometer was successfully used to record XANES spectra of several classes of materials in condensed state [12, 18, 19]. This instrument is equipped with an optical system for focusing monochromatic X rays based on the Johannson method. We recorded the Ti *K*-edge XANES spectra in a test compound (rutile) and the Fe *K*-edge XANES spectra in the garnet under study. XANES spectra were recorded in the transmission mode [20]. The current through the X-ray tube was 100 mA at a voltage of 10 kV (when recording the Ti *K*-edge spectra of rutile) and 20 kV (for the Fe *K*-edge spectra of garnet). We used a molybdenum cathode and a Ge(220) crystal as a monochromator. An Ar-300 gas detector was used to record the incident X-ray intensity. The X-ray intensity transmitted through the sample was recorded using a SC-70 scintillation detector. The titanium *K* edge spectra of rutile were recorded in a range of 4940–4956 eV and above 5050 eV with a step of 2 eV, in a range of 4956–5000 eV with a step of 0.5 eV, and in a range of 5000–5050 eV with a step of 1.0 eV. The iron *K* edge spectra of garnet were recorded in a range of 7070–7090 eV and above 7150 eV with a step of 2.0 eV and in a range of 7090–7150 eV with a step of 1.0 eV. X-ray absorption spectra were averaged over four scans.

CALCULATION TECHNIQUE

The Fe *K*-edge XANES spectra of garnet were theoretically analyzed based on two methods: the full multiple scattering theory within a muffin-tin approximation for the potential shape (using the FEFF8.2 code [21, 22]) and the full-potential finite difference method (using the FDMNES code [23]).

Calculations using the FEFF8.2 code were based on the formalism of the Green's function in real space. When determining the crystal potential, free-atom potentials are initially calculated using the relativistic Dirac–Fock model for each type of atom. The electron density in a cluster under consideration then is constructed by partial overlap of free-atom densities within the muffin-tin approximation [7], after which the exchange part in the form of the Hedin–Lundqvist potential is taken into account. In the next stage, the crystal potential is self-consistently determined on the basis of an iterative cycle and the phase shifts of scattering and dipole matrix elements of transitions are calculated. The phase shifts of scattering are determined on muffin-tin spheres, and the relativistic dipole-matrix elements of transition are determined using the continuous-spectrum and core wave functions. Full multiple-scattering calculations are performed for a chosen cluster around the central absorbing atom.

FDMNES calculations were carried out on the basis of the well-known finite difference method, which is widely used to solve numerically differential equations. In this technique, an equation is solved on a calculation grid. In the case of XANES spectra, the object of interest is the Schrödinger equation for a rather large region around an absorbing atom. FDMNES calculations are performed in the "full" potential (beyond any approximation for the potential shape), thus avoiding the problem related to the classical muffin-tin approximation. The potential is determined using the exchange Hedin–Lundquist potential.

Chemical composition of garnet from placer deposits of the Taman peninsula (normalized to 100%), obtained with an Oxford INCA Energy 450/XT energy-dispersive X-ray fluorescence microanalyzer (with measurements at 27 points)

Component	Content (wt %)	Mean square deviation
SiO_2	35.36	0.17
Al_2O_3	20.97	0.29
FeO_{sum}	34.93	0.87
MnO	6.62	0.81
MgO	1.54	0.28
CaO	0.58	0.08
Total	100.00	

All the spectra reported here were calculated taking into account the core hole.

RESULTS AND DISCUSSION

The end members of the isomorphous series of natural garnets are andradite $Ca_3Fe_2(SiO_4)_3$, almandine $Fe_3Al_2(SiO_4)_3$, grossular $Ca_3Al_2(SiO_4)_3$, uvarovite $Ca_3Cr_2(SiO_4)_3$, pyrope $Mg_3Al_2(SiO_4)_3$, and spessartine $Mn_3Al_2(SiO_4)_3$.

In the first stage of our study, we determined the qualitative elemental composition of the garnet deposit of the Taman peninsula by recording X-ray fluorescence spectra on an analytical short-wavelength SPARK-1-2M X-ray spectrometer. A high content of iron was revealed in the sample.

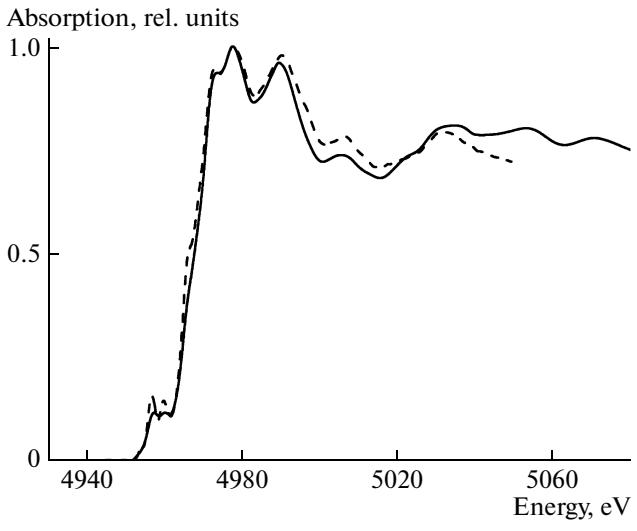

Fig. 1. Comparison of the experimental Ti *K*-edge XANES spectra of rutile recorded on a laboratory Rigaku R-XAS spectrometer (solid line) and the SLS synchrotron source [24] (dashed line).

Quantitative X-ray fluorescence analysis (Oxford INCA Energy 450/XT microanalyzer) was performed on grains with previously confirmed phase and chemical homogeneity. The proximity of the garnets studied to the pyrope–almandine–spessartine series, which is characterized by relatively low calcium content, was established (see table). Since the valence state of iron cannot be established by X-ray fluorescence analysis, it is impossible to correctly estimate the concentrations of iron-containing almandine ($Fe_3^{2+}Al_2(SiO_4)_3$) and andradite $Ca_3Fe_2^{3+}(SiO_4)_3$ minals, which are considered to be end members of isomorphous garnet series.

In the next stage, the garnet sample was studied by analyzing the X-ray absorption spectra. First, the Ti *K* XANES spectrum of the test compound rutile (TiO_2) was recorded using a laboratory Rigaku R-XAS spectrometer. Comparison of the experimental Ti *K*-edge XANES spectrum of rutile recorded on a laboratory Rigaku R-XAS spectrometer with the spectrum obtained for a similar sample on a synchrotron radiation source (Swiss Light Source (SLS), Switzerland) [24] showed their agreement (Fig. 1), which indicates that the resolution of the laboratory Rigaku R-XAS spectrometer is quite sufficient for measuring X-ray spectra of geological materials. According to the X-ray fluorescence data, the garnet sample under study is characterized by high iron content; therefore, analysis was concentrated on the Fe *K*-edge XANES spectrum.

Theoretical analysis of the Fe *K*-XANES spectrum of the garnet was done for two iron-containing garnet representatives: almandine and andradite. Almandine and andradite belong to the cubic system of space group *Ia3d* with lattice parameter $a = 11.531$ Å for almandine and 12.058 Å for andradite [25]. The theoretical spectra were obtained by two methods: full multiple scattering with a muffin-tin potential using the FEFF8.2 code and the full-potential finite difference method using the FDMNES code. Full multiple-scattering calculations were performed for atomic clusters containing 400 and 369 atoms for almandine and andradite, respectively. The finite difference method calculations of XANES spectra were carried out for an atomic cluster 5.3 Å in radius around a central absorbing iron atom; the cluster consisted of 59 and 57 atoms for almandine for andradite, respectively. The experimental Fe *K*-edge XANES spectrum of the garnet is compared with the theoretical spectra calculated for almandine and andradite based on the finite difference method (FDMNES code) in Fig. 2. One can conclude that the spectrum calculated for the structural model of almandine is in better agreement with the experimental Fe *K*-edge XANES spectrum of the garnet sample under study. The theoretical spectrum calculated for the almandine model reproduces

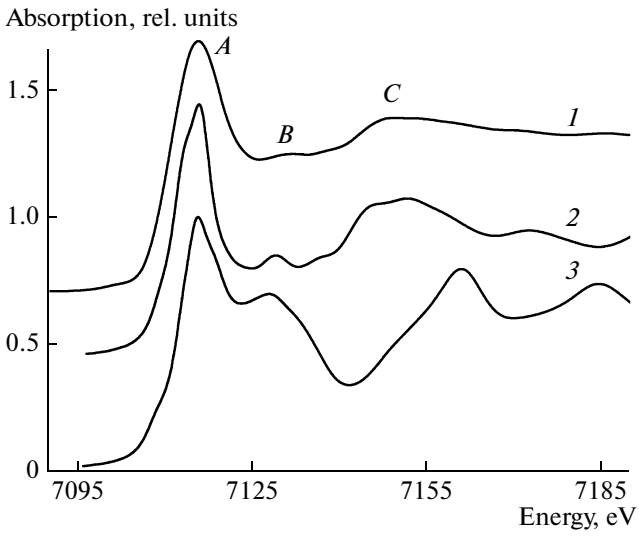

Fig. 2. Comparison of the (*1*) experimental Fe *K*-edge XANES spectrum of garnet from the Taman peninsula with the theoretical spectra calculated for (*2*) almandine and (*3*) andradite based on the fullpotential finite difference method using the FDMNES code.

all the features of the experimental spectrum and is in agreement with the experimental data with respect to the energy positions of peaks. At the same time, the shape of the spectrum calculated for the andradite model deviates from the experimental one, for example, concerning the energy position of the feature denoted as *C*.

Similar results were obtained when calculating the XANES spectra for almandine and andradite based on the full multiple-scattering method (FEFF8.2 code). When calculating the component composition of garnets based on X-ray fluorescence data and on the assumption of divalent state of iron, the content of andradite ($Ca_3Fe_2^{3+}(SiO_4)_3$) minal did not exceed 0.15%, which also confirms the agreement of the experimental data with the theory for the almandine model. Thus, the analysis of the Fe *K*-XANES spectra indicates that the almandine component is dominant on the composition of the garnet from the recent placer deposit of the Taman peninsula. These results are in agreement with the mineralogical data [26].

CONCLUSIONS

We investigated garnet samples selected from recent magnetite–garnet placer deposits of the Taman peninsula. The analysis of their X-ray fluorescence spectra showed that these garnets have high iron content and belong to the pyrope–almandine–spessartine series. The Fe *K*-edge XANES spectra of the garnet samples were recorded on a laboratory Rigaku R-XAS X-ray absorption spectrometer. Comparison of the experimental Fe *K*-edge XANES spectrum with the theoretical spectra calculated for the iron-containing minals of the isomorphic garnet series (almandine—$Fe_3^{2+}Al_2(SiO_4)_3$ and andradite—$Ca_3Fe_2^{3+}(SiO_4)_3$) showed that the garnets of the Taman placer deposits belong to almandines.

On the whole, our study has demonstrated that XANES spectroscopy allows one to obtain information on the local atomic structure of natural minerals, including those characterized by complex isomorphous substitutions.

REFERENCES

1. A. J. Berry, L. V. Danyushevsky, H. St. C. O'Neill, M. Newville, and S. R. Sutton, Nature **455**, 960 (2008).
2. A. J. Berry, G. M. Yaxley, A. B. Woodland, and G. J. Foran, Chem. Geol. **278**, 31 (2010).
3. A. J. Berry, A. M. Walker, J. Hermann, H. St. C. O'Neill, G. J. Foran, and J. D. Gale, Chem. Geol. **242**, 176 (2007).
4. A. M. Walker, J. Hermann, A. J. Berry, and H. St. C. O'Neill, J. Geophys. Res. **112**, B05211 (2007).
5. I. Ya. Nikiforov, *Interaction of X Rays with Matter* (DGTU, Rostov-on-Don, 2011) [in Russian].
6. G. Bunker, *Introduction to XAFS: A Practical Guide to X-Ray Absorption Fine Structure Spectroscopy* (Cambridge Univ. Press, Cambridge, 2011).
7. J. J. Rehr and R. C. Albers, Rev. Mod. Phys. **72**, 621 (2000).
8. A. V. Soldatov, J. Struct. Chem. **49**, S102 (2008).
9. A. V. Soldatov, G. Yu. Smolentsev, A. N. Kravtsova, V. L. Mazalova, I. E. Shtekhin, and T. S. Belikova, Zavod. Lab. Diagn. Mater. **74** (10), 28 (2008).
10. G. Smolentsev and A. Soldatov, J. Synch. Radiat. **13**, 19 (2006).
11. A. N. Kravtsova, G. E. Yalovega, A. V. Soldatov, W. S. Yan, and S. Q. Wei, J. Alloys Compd. **469**, 42 (2009).
12. A. A. Guda, N. Smolentsev, J. Verbeek, E. M. Kaidashev, Y. Zubavichus, A. N. Kravtsova, O. E. Polozhentsev, and A. V. Soldatov, Solid State Commun. **151**, 1314 (2011).
13. M. A. Bryleva, A. N. Kravtsova, I. N. Shcherbakov, S. I. Levchenkov, L. D. Popov, V. A. Kogan, Yu. P. Tupolova, Ya. V. Zubavichus, A. L. Trigub, and A. V. Soldatov, J. Struct. Chem. **53** (2), 295 (2012).
14. N. D. Tailby, A. M. Walker, A. J. Berry, J. Hermann, K. A. Evans, J. A. Mavrogenes, H. St. C. O'Neill, I. S. Rodina, A. V. Soldatov, D. Rubatto, and S. R. Sutton, Geochim. Cosmochim. Acta **75**, 905 (2011).
15. I. S. Rodina, A. N. Kravtsova, M. A. Soldatov, A. V. Soldatov, and A. J. Berry, J. Phys.: Conf. Ser. **190**, 012181 (2009).
16. I. S. Rodina, A. N. Kravtsova, A. V. Soldatov, and A. J. Berry, Opt. Spectrosc. **111** (6), 936 (2011).
17. http://www.nanospectr.sfedu.ru.

18. A. A. Guda, S. P. Lau, M. A. Soldatov, N. Yu. Smolentsev, V. L. Mazalova, X. H. Ji, and A. V. Soldatov, J. Phys.: Conf. Ser. **190**, 012136 (2009).
19. M. A. Evsyukova, G. Yalovega, A. Balerna, A. P. Menushenkov, Ya. V. Rakshun, and A. A. Teplov, Phys. B **405**, 2122 (2010).
20. G. V. Fetisov, *Synchrotron Radiation: Methods for Structural Studies of Materials* (Fizmatlit, Moscow, 2007) [in Russian].
21. A. L. Ankudinov, B. Ravel, J. J. Rehr, and S. D. Conradson, Phys. Rev. B **58**, 7565 (1998).
22. A. L. Ankudinov, C. E. Bouldin, J. J. Rehr, J. Sims, and H. Hung, Phys. Rev. B **65**, 104107 (2002).
23. Y. Joly, Phys. Rev. B **63**, 125120 (2001).
24. A. N. Kravtsova, A. V. Soldatov, M. Nachtegaal, M. W. Tew, and J. A. van Bokhoven, Phys. B **405**, 724 (2010).
25. G. A. Novak and G. V. Gibbs, Am. Mineral. **56**, 791 (1971).
26. N. I. Boiko and A. V. Korkoshko, Izv. Vyssh. Uchebn. Zaved., Geol. Razvedka, No. 1, 22 (2007).